Low Energy (<10 eV) Electron Collision with Benzonitrile-CCl4 Admixture: A Combined Theoretical and Experimental Study

H. Abdoul-Carime, Guillaume Thiam, Franck Rabilloud

Low Energy (< 10 eV) Electron Collision with Benzonitrile-CCl_4 Admixture: A Combined Theoretical and Experimental Study

H. Abdoul-Carime [1*], Guillaume Thiam [2,3], Franck Rabilloud [2]

[1] Universite Claude Bernard Lyon 1, Institut de Physique des 2 Infinis, CNRS/IN2P3, UMR5822, F-69003 Lyon, France

[2] Universite Claude Bernard Lyon 1, CNRS, Institut Lumière Matière, UMR5306, F-69622 Villeurbanne, France

[3] Dipartimento di Chimica, Biologia e Biotecnologie,

Università degli Studi di Perugia, Via Elce di Sotto, 8,06123, Perugia, Italy

*Corresponding author: hcarime@ipnl.in2p3.fr

ABSTRACT

Benzonitrile (BZN) and carbon tetrachloride (CCl_4) are versatile solvents used as a precursor for the synthesis of many products. As ~~a~~ multi-usage molecules, these compounds may be involved in sustainable chemistry processes such as the cold plasma techniques for which the generated electrons are known to be responsible for reactions. Therefore, it is desirable to explore the interaction of low energy electrons with the co-compounds in the gas phase. The production of chlorine and cyanine anions, initiated by the electron collision with CCl_4 and BZN, respectively, undergo nucleophilic substitution S_N2 reaction with the precursors molecules for the synthesis of chlorobenzene and tricholoacetonitrile. The mechanism of fragmentation of benzonitrile and the synthesis reactions are rationalized by DFT calculations. The yield of the cyanine anion produced from the ion reaction increases with the temperature of the admixture gas, probed in the 25 °C-100 °C temperature range. The present work may contribute to a potential process for the production of chlorobenzene for instance via (cold) plasma techniques.

I. INTRODUCTION

Benzonitrile (BZN) contains a cyano (CN) group conjugated with a phenyl moiety, for which the activation of the C-CN bond plays an important role in synthesis. BZN is a widely known solvent used as a precursor in industries for drugs, perfumes, dyes, rubber, or resins [1]. For instance, the benzoic acid, used as a preservative or fragrance additive in cosmetics, is synthesized from BZN by reacting with H_2O, leading to the alteration of the CN moiety for the COOH group. Recently, BZN has been detected in space [2], opening the perspective for this molecule to be a fundamental building block for complex space chemistry leading to larger polyaromatic hydrocarbons [3,4] or polyaromatic nitrogen heterocycles [5]. In the interstellar environment, the chemistry of BZN may be operated via a photo-dissociation process, as the first step, by VUV lights yielding the phenyl, C_6H_5, and the cyano, CN, radicals [6]. These sub-products further react leading to more complex species. The interstellar chemistry may also be triggered by the energetic primary particles (e.g., cosmic rays, ..). However, in dense environments or solid media such as ices, the primary particles generate a large number of secondary species among which, are ballistic electrons [7] with an energy distribution below 10 eV [8]. Therefore, ballistic secondary electrons also play a role in the interstellar chemistry [9], and the reaction of BZN in water ice environment producing phenol, via the dissociation of the C-CN bond triggered by low energy electrons has been recently observed [10].

The ability of the free low-energy electrons to induce chemistry has now been demonstrated [11,12]. For instance, it has been shown that these particles are able to produce large hydrocarbons from methanol ices [13] or they can induce reaction selectivity even at very low energies (< 5 eV) [14]. More recently, the chemistry promoted by plasmonic “hot electrons”, produced when a metal surface is excited by light in the visible range [15,16], has seen a strong increase of interest, particularly in the field of catalysis [17,18] and nanoscale chemistry and engineering [19,20]. These “hot” carriers, with an energy distribution below few eVs [13,21], are capable of driving catalytic reactions. Another source of low energy electrons [22] concerns the emerging cold plasma technologies [23] in which the ionization of the gas produces electrons that participate to the synthesis reaction at low temperatures, e.g., < 100 °C. Therefore, understanding and quantifying the intrinsic electron-molecule processes is desirable for a better comprehension of chemistry at the surface, in plasma technologies, or in high-density interstellar environments.

The first part of this contribution thoroughly discusses the process implicated in the fragmentation of benzonitrile [24] by low energy electrons and more particularly, the dissociation channel leading to the cleavage of the C-CN bond. This work is supported by a combined recent

developed state-of-the-art TDDFT theory [25] and experimental technique. The cyanide CN^- anion is formed via a resonant electron induced process for which the involved molecular orbitals are calculated. Moreover, the production cross-section of this anion is estimated by calibrating with the one of the Cl^- anion from carbon tetrachloride, CCl_4, for which the absolute formation cross-section is well established [26]. Finally, it has been observed that the presence of the calibration molecule in the BZN gas generates the chlorine Cl^- anions that further react with BZN molecules, leading to the production of the cyanide anions near 0 eV, conjointly with the chlorobenzene counterpart. The CN^- anions produced via the ion reaction increases with the temperature of the admixture gas.

II. METHODOLOGIES

Theoretical Method

Calculations have been performed in the framework of the density-functional theory (DFT) and the time-dependent DFT (TDDFT). The resonance electron attachment energies are calculated with a multi-basis-set TDDFT method [23]: the vertical electron affinity (VEA) is evaluated using DFT calculations with the diffuse basis set aug-cc-pvtz [27] while the anionic excitation energies are calculated using TDDFT and the cc-pvtz basis set. The exchange and correlation potential is that of the range-separated hybrid density functional ωB97x [28]. The use of the relatively small basis set cc-pvtz (without any diffuse function) is well suited to describe valence-type excitations while preventing the occurrence of intruder discretized continuum states [23]. All calculations are performed with the Gaussian16 suite of programs [29]. Pre- and postprocessing operations are performed by using the graphical interface Gabedit [30].

Experimental Method

The experimental setup has been thoroughly described elsewhere [31,32]. Only the essential of the method will be provided here. The cross-beam experiment, working at ultra-high vacuum conditions (base pressure of 6.10^{-9} mbar), is composed of a molecular beam, a double counter-propagating electron beams produced by two electron guns (EG1 and EG2) and a dual (+/-) time-of-flight mass spectrometer, all mounted orthogonally. EG1, equipped with a trochoidal monochromator, based on a dispersive **ExB** field, provides a mono-kinetic electron beam of about 10 nA with an energy resolution of 350 meV. EG1 is used for inducing the electron-molecule collision experiments. The role of the EG2 is to ionize the parent molecule or fragment

formed after the fragmentation of the precursor, if necessary. A dual (+/-) time-of-flight mass spectrometer (TOF-MS) detects the negative and the ionized neutral species that are produced after the collision of the target molecule with electrons from EG1 or/and EG2. The negative and positive ions are expelled from the collision area by a -450 V and 600 ns pulse, and they are accelerated by +1450 V and -2000 V respectively (acceleration area), before reaching the free field zone for the time separation. They are collected by a pair of multi-channel plates (MCPs) transforming the arriving ions to electric pulses. These are *in fine* stored in a PC for 'off line' analysis. Note that with this experimental arrangement, it is possible to systematically verify the molecular beam (e.g., purity of the investigated product, etc.) prior to further electron collision studies.

III. RESULTS

Two series of experiments were undertaken: (1) a pure molecular beam of BZN and, (2) an admixture beam of BZN with CCl_4 (1:2) pre-mixed in a mixing chamber, are injected for the collision experiments. The advantage of this latter procedure (i.e. pre-mixed molecules) is two-fold: mass calibration of the fragments from the dissociation of BZN induced by the electron collision, and, the direct comparison of the intensity of the produced anion yields, which provide the fragmentation cross-section as it will be discussed in the following. On the other hand, reactions induced by the ions, formed from the calibration molecules, may arise. Indeed, it has already been reported such ion-molecule reactions in low-energy electron-molecule collision experiments in which the investigated molecule coexists with the calibration gas (SF_6 [33] or CCl_4 [24]) in the molecular beam.

Figure 1 shows the mass spectra recorded at different electron accelerating voltages (AV1): (a) 0.5 V, (b) 0.9 V, (c) 3.7 V, and (d) 7.3 V. In this experience, the molecular beam consists of an admixture of BZN:CCl_4 (1:2). Mass spectrum recorded at the AV1 value of 0.5 V shows only background noise (Fig. 1a). As the AV1 increases (Fig.1b-d), a signal at m/z of 35 (a.u.) can be observed, followed by an additional fragment detected at m/z of 26 (a.u.). The second anion species is attributed to the CN^- anion, while the first anion is associated to the chlorine $^{35}Cl^-$ anion for which its isotopic counterpart, i.e., $^{37}Cl^-$, is also clearly observed. A further fragment is clearly observed at m/z 77 amu (i.e., $C_6H_5^-$) for the AV1 of 7.3 V, as well as a tiny feature at m/z 102-103, which could be associated to the $(BZN\text{-}H)^-$ anion (Fig. 1d). These results confirm the previous work [22] in terms of the production of the anion fragments. On the other

hand, the observation of the CN^- anion production at very low electron acceleration voltage (i.e., 0.9V) is quite surprising.

The potential energy curves (PECs) of the neutral BNZ (purple) and the BZN^- anion (black), calculated at the ωB97x/cc-pvtz level of theory, are plotted as the function of the C-CN bond elongation are (Fig.3). The anion PEC exhibits a potential barrier of 0.3 eV. In Figure 4, the molecular orbitals of the BNZ^- anion are shown and the electron attachment energies are provided. The energetics of the fragmentation calculated at the ωB97x/aug-cc-pvtz level of theory are provided in Table 1.

In the following, we will concentrate specifically in the production of the cyanide anion. At a given AV1 value, the CN^- anion yield is obtained by integrating the mass spectrum at the specific m/z value and by subtracting the respective background noise. This integrated yield is then normalized to the transmitted electron current. Figure 2 exhibits the yield of the CN^- anion fragment as the function of the electron accelerating voltage, AV1. The solid blue line corresponds to the yield obtained from the electron collision with pure BZN gas, while the dashed blue line corresponds to measurements with mixed BZN/CCl_4 gas. In the inset of Fig.2, the yield function of the CN^- and Cl^- anions are normalized to the maximum of their respective yield. As the Cl^- anion is well known to be produced at ~0 eV incident electron energy [34], the electron energy scale is obtained by shifting the AV1 scale by 0.4 V. Thus, the first peak in the CN^- yield function (solid blue line) is observed with an electron attachment energy of 2.85 eV agreeing well the previous report [24].

IV. DISCUSSION

The CN^- anion yield function (Fig. 2) exhibits peaked features reminiscent of resonant fragmentation processes. At these energies, dissociative electron attachment, DEA, is the efficient mechanism for molecular dissociation [35]. In brief, the colliding electron is captured by the target molecule to form a transitory negative anion which undergoes dissociation into a negative anion and at least one neutral species. The fragmentation cross-section, related to the intensity of the measured anion signal, is a convolution of the electron capture cross-section, σ_{capt}, with the survival probability P_s [35,36]. While σ_{capt} reflects the capture of the electron process, P_s depends on the dissociation lifetime vs. the electron auto-detachment time [35,36]. The dissociation time corresponds to the time for the C-CN bond to reach the crossing of the neutral (purple) and anion (black) potential energy curves (Fig.3). The capture of the colliding electron

may arise via (a) the shape resonance, i.e, the accommodation of the excess electron into an unoccupied virtual molecular orbital (MO), (b) core excited resonance (i.e., excitation of a core electron into an empty molecular orbital, while the excess electron being captured by the positive core) and, (c) Feshbach resonance mediated by di-(multi)pole bound anion formation [37,38]. The formation of the temporary anion π* states via shape resonance has been observed by the electron transmission spectroscopy, ETS, [39].

For the benzonitrile, the calculated electron attachment energies together with the orbital of the excess electron is shown in Figure 4. The first two resonances are attributed to π* states, the first one at 0.20 eV is expanded on both phenyl and cyano parts, while the second, at 0.96 eV, is localized on the phenyl moiety. These states do not present a dissociative character therefore no anion fragment can be formed and detected. The calculated 0.96 eV state agrees well with the ETS measurements [39]. The fact that the BNZ^- anion has not been detected here and in the previous report [24] suggests that electron-autodetachment time is shorter than the dissociation time. Above 3 eV, several resonant states, where the extra electron is mainly localized on the CN group, are predicted (3.24, 3.86, 5.08 eV, etc.). In particular, the resonance at 3.24 eV is due to the attachment of the electron on CN in a π* orbital. The dissociation of the BZN^- transitory anion into a CN^-anion and a phenyl radical fragments presents a barrier energy of 0.3 eV, as shown in Figure 3. However, the true barrier is expected to be inferior as the local relaxation of both phenyl and cyanide groups should be considered. Then, the formation of the anion CN^- is very likely near 3-3.5 eV. We have performed a local optimization of the BZN^- anion in this excited state and found a state located 0.5 eV below (the main structural changes are a small elongation, from 1.148 to 1.236 Å, of the C-N bond length, and a shortening, from 1.437 down to 1.418 Å, of the C-CN bond length). This state lies only 2.74 eV above the ground state of the neutral molecule. Therefore, the resonance calculated at 3.24 eV (vertical transition) or 2.74 eV (adiabatic transition) is associated to the broad experimental peak located at 2.85 eV, bearing in mind that the observed peak position is a convolution of the capture cross section (MOs state) and the survival probability, which are both energy dependent [35,36]. Further features are experimentally observed at 3.95 eV (shoulder), 5.54 eV and 7.05 eV (**SI1**). They can be associated to the MOs calculated at 3.86 eV and 5.08-6.11 eV and shown in Fig. 4. From the calculations, the shape- and core-excited resonances co-exist in the energy range of 4.48 – 5.7 eV. At higher energies, around ten excited states are calculated between 6 and 8 eV, they may be associated to the fragmentation of the parent temporary anion into the CN^- anion observed in the experiment (broad peak around 7 eV). The

present observation agrees in some degrees that of Heni et al. [24], albeit they have reported an unresolved feature in the [6-8] eV range.

The energy threshold for the production of the CN^- anion, the $(BZN-H)^-$ and the $C_6H_5^-$ anion fragments are calculated to be 2.06, 3.18 and 5.21 eV respectively (Table 1 a,b and c). For the cyanide anion, the experimental production threshold is slightly lower than the prediction (c.a., 1.3eV). The production of the $C_6H_5^-$ anion can only arise at incident electron energies above 5.21 eV in agreement with the previous work [24]. As discussed above, not only the energetics of the reaction but also the resonance state and the dissociation time vs. autodetachment time control the dissociative electron attachment, i.e., the anion fragment production. The anion production cross section, $\sigma_{ion}(E)$, at a given incident electron energy, E, can be estimated via $N_{ion}(E) = \varepsilon.N_e.N_{neutral}.\sigma_{ion}(E).L$, where N_{ion} represents the number of collected ions, ε the detection efficiency, N_e and $N_{neutral}$ the number of colliding electrons and the density of the neutral target molecules, respectively, and L the length of the interaction region. Since $N_{neutral}$ and L are not accessible, $\sigma_{CN^-}/\sigma_{Cl^-}$ can be obtained by knowing the gas pressure ratio, P_{BZN}/P_{CCl4} (i.e., ½ in the present work), and the measured numbers of ions N_{CN^-}/N_{Cl^-} (c.a., $2.59\ 10^{-2}$). From the yield functions of the Cl^- and CN^- anions (solid dashed and green lines, Fig. 3) and with the known σ_{Cl^-} at ~ 0 eV (c.a., 10^{-13} cm^2 [34]), the cross-section for the production of the cyanide anion can be estimated at the electron energy of 2.85 eV to be 5.10^{-15} cm^2, while at 7.07 eV it is found to be 40% larger.

As it can be seen in Fig.2, i.e., the dashed and the solid blue lines, the co-presence of the calibration molecules, CCl_4, in the molecular beam under electron impact leads clearly to the appearance of an additional feature in the CN^- anion yield function, peaked at 0.4 eV with a threshold at ~0.1 eV. Since at such low energies, only the chlorine anion can be produced with an appreciable cross-section via the dissociation of the transitory $CCl_4^{\#-}$ precursor anion [34], this present observation indicates the reaction of the produced Cl^- and potentially the $CCl_4^{\#-}$ anions with the neutral BZN molecules yields the CN^- fragment anion. Such a S_N2 nucleophilic substitution reaction has already been observed earlier in DEA to thymine or adenine experiments when the calibration gas (i.e., CCl_4 or SF_6) is introduced simultaneously with the studied molecules [40,41]. It is to be noted that for the suggested Cl^- ion reaction with thymine (T) yielding the $(T-H)^-$ negative ion fragment, the (T-H) radical electron affinity of the target molecule is high (c.a., 3.4 eV [42]). In the present work, the high electron affinity of the cyano radical (c.a., 3.86 eV [43]) also leads to such an ion reaction.

To support our observations, we have performed different fragmentation scenarios presented in Table 1d-f. The lowest reaction energy corresponds to the capture of the colliding electron by the CCl_4 target to form the transitory $CCl_4^{\#-}$ anion, the transfer of the extra charge to BZN, which dissociates into the fragment CN^- negative species concomitantly with the formation of the chlorobenzene, ClC_6H_5, molecule. The lifetime of the transitory tetrachloride anion is short (7.5 ps and 10-30 ps) [44], suggesting that the two partners must be sufficiently close for such reaction to arise. The calculated Gibbs energy at 300 K of 0.02 eV is in relatively good agreement with the CN^- production threshold of ~0.1 eV (Fig. 2, dashed line). The second most accessible reaction (Table 1f) corresponds to the formation of the Cl^- negative fragment via DEA to CCl_4. It is then this chlorine anion that further reacts with BZN for the concomitant production of the CN^- anion and the ClC_6H_5 , chlorobenzene, molecule. The calculated energy threshold at 300 K is higher (1.28 eV) but the reaction is nevertheless accessible. The reaction (g) leading to the formation of BZN^- parent anion requires at least 3.8 eV. At such energies, the BZN^- anion produced by the charge transfer process is likely to fragment since the excess electron may occupy some of the dissociative states calculated above.

Another possible ion reaction involves the CN^-, anion produced via DEA to BZN with CCl_4 present in the admixture. Such a reaction listed in Table 1h may arise since the high electron affinity of the CN radical, similarly to previously discussed for the Cl^- anion induced reaction. Therefore, the very exothermic reaction (h) in Table 1 suggests that a relatively good efficiency for the production of CCl_3CN, tricholoacetonitrile as experimentally observed in in **SI2**.

The production yield of the Cl^- anion at electron energy of about ~ 0.5 eV is almost unchanged in the 20-130 °C temperature range, in agreement with previous study [45] (Fig.5a, open squares). In contrast, temperature dependence of the CN^- anion yield presents two features (Fig. 5a, solid circles). At temperatures below 60 °C, the yield presents a stable value, while above, an increase is observed. The production the CN^- anion at near 0 eV arises from S_N2 for which the temperature dependence is related to the Arrhenius activation energy [46]. As the gas pressure is kept constant during the measurements, these findings indicate that the ion reaction cross section must increase. The yield ratio (CN^-/Cl^-) suggests an increase in the ion reaction efficacy by almost 3-4 in the 60-130 °C temperature range (Fig. 5b).

V. CONCLUSION

The dissociation of benzonitrile induced by electron at low energies (< 10 eV) analyzed by time-of-flight mass spectrometry shows the production of the CN^- anion fragments, via

dissociative electron attachment. DEA is a convolution of the electron capture process and the (temporary anion) survival probability, the anion states have been explored by TD-DFT theory. In presence of the calibration gas CCl_4, the ion reaction is observed to arise from the production of the cyanide anion. Two reactions representing the most probable mechanisms have been determined: (1) $CCl_4^{\#-}$ + BZN and (2) Cl^- + BZN, for which (1) has the lowest energy threshold. Both processes produce chlorobenzene along with the cyanide anion. Another ion-reaction arises from the formed CN^- anion from DEA to BZN, with CCl_4, yielding tricholoacetonitrile, CCl_3CN.

In this work, it has been shown that both C_6H_5Cl and CCl_3CN result from the S_N2 reactions initiated by the collision of an admixture of CCl_4-BZN with low energy electrons. The production of chlorobenzene may be of particular interest since the compound is involved in the manufacturing of many industrial products (rubber, paint, adhesive), and the industrial demand is incearsing according to the chlorobenzene market forecast [47]. The compound is industrially produced by the Raschig-Hooker method for which the benzene vapors hydrogen chloride and oxygen are catalyzed on copper oxide at 250 °C under a continuous flow. The present findings may suggest an alternative process for preparing chlorobenzene from an admixture of benzonitrile and carbon tetrachloride via cold plasma at low temperatures (60-130 °C). For the trichlorobenzene, known to be a precursor of etridiazole, a commercially used fungicide, is obtained from many processes among which the chlorination of acetonitrile at high temperatures (200-500 °C) in presence of catalysts, or photochlorination. Here it has been shown that this compound is generated from the electron collision at low energies with carbone tetrachrloride-benzonitrile admixture.

As benzonitrile is a solvent used as a precursor for the synthesis of a large spectrum of products, the detailed understanding of fragmentation of the molecule by low energy electrons may potentially help for the development of future chemistry processes involving (hot) electrons such as the catalysis by solar light [48], green chemistry [49,50] or industrially scalable cold plasma technology[51].

VI. ACKNOWLEDGMENTS

This study was supported by the ANR-PRC-BAMBI (grant number 18-CE30-0009-03). In addition, F.R. thanks the GENCI-IDRIS for supporting the computing time through the grant (A0130807662) and the Pôle Scientifique de Modélisation Numérique (PSMN).

VII. TABLES

Table I. Energy (in eV) for the production of anion and corresponding neutral fragment, calculated at ωB97x/aug-cc-pvtz level of theory. Gibbs free energy at 300 K is given in parenthesis.

Reaction	**Fragmentation Energy (eV)**
(a) BZN → CN^- + C_6H_5	2.06
(b) BZN → $(BZN-H)^-$ +H	3.18
(c) BZN → $C_6H_5^-$ + CN	5.21
(d) CCl_4 + BZN → CN^- + ClC_6H_5 + CCl_3	0.68 (0.02)
(e) CCl_4 + BZN → CN^- + Cl + C_6H_5 + CCl_3	4.21
(f) Cl^- + BZN → CN^- + ClC_6H_5	1.47 (1.28)
(g) Cl^- + BZN → Cl + BZN^-	3.83
(h) CN^- + CCl_4 → Cl- + $CNCCl_3$	-1.20 (-1.06)

VIII. FIGURES

FIGURE 1: Mass spectra of anion recorded at the electron accelerating voltage, AV1 of (a) 0.5 V, (b) 0.9 V, (c) 3.7 V, and (d) 7.3 V. The dashed lines are guides-to-the eyes.

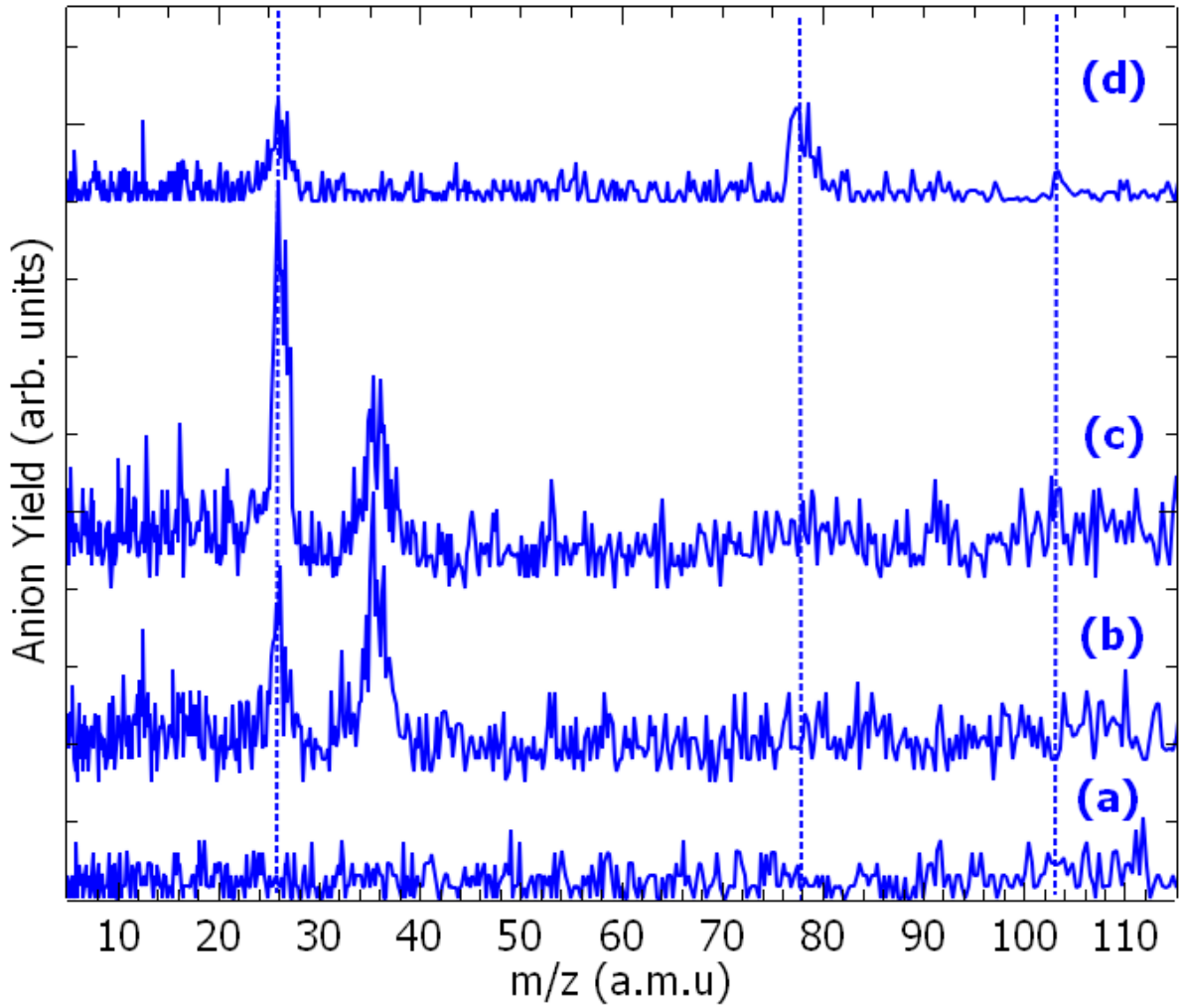

FIGURE 2: CN^- anion yield as the function of the Electron Accelerating Voltage (V) for the electron collision with pure benzonitrile (BZN) gas (solid blue) and mixed BZN:CCl_4 gas (dashed blue). In the inset the anion yield functions are obtained from electron impact on pure CCl_4 and BZN vapors. The yield the Cl^- (solid green) and the CN^- (solid blue) anions normalized to the respective maximum value are plotted as the function the Electron Accelerating Voltage (AV1). The maximum and the FWHM in the Cl^- anion yield provide the 0 eV and the energy resolution of the electron beam [33]. The first peak in the CN^- yield function is observed with an electron attachment energy of 2.85 eV.

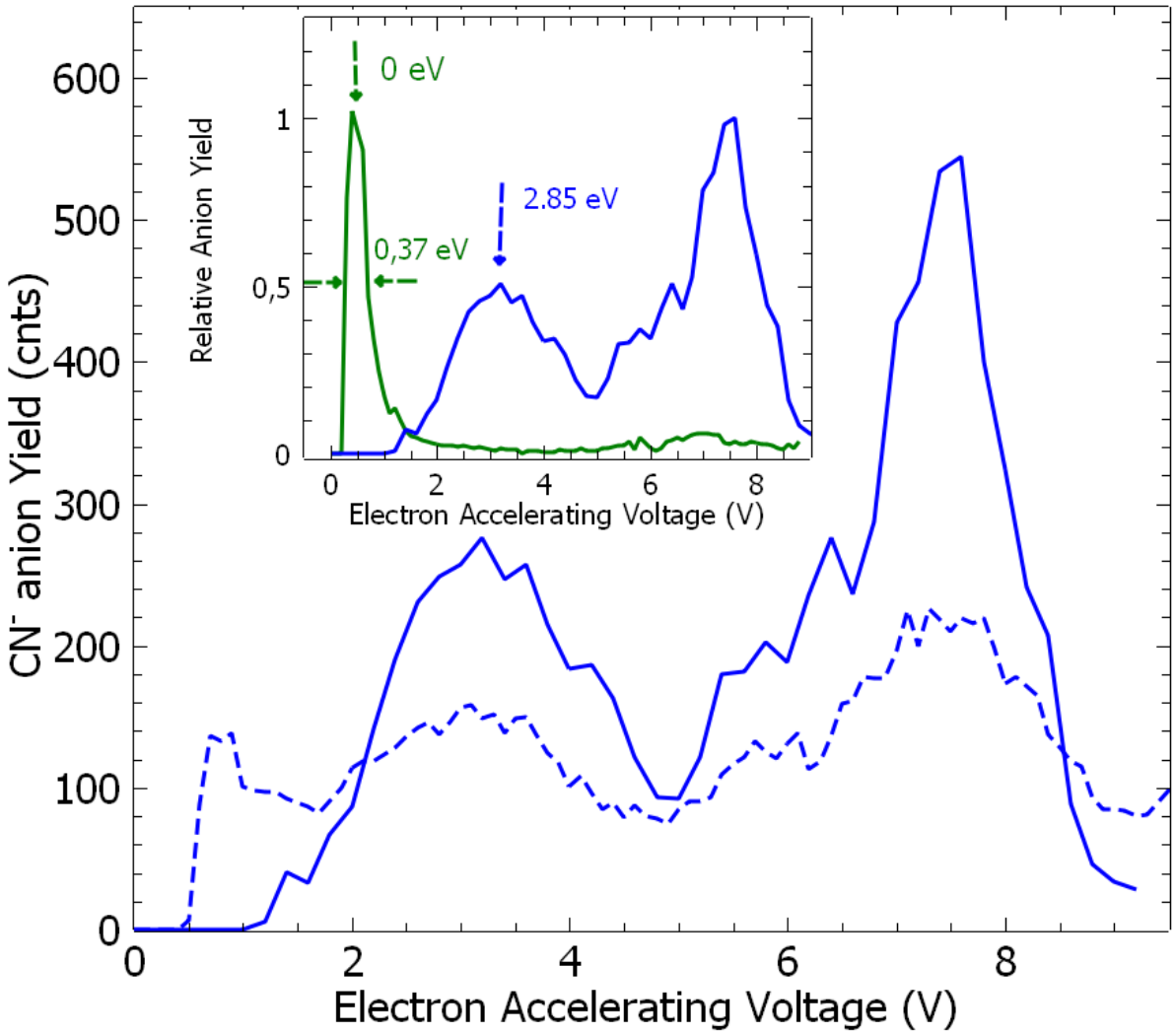

FIGURE 3: Potential energy curves of the neutral BZN and the anion BZN^- as a function of the C-CN bond elongation in Å, 0 refers to the equilibrium distance in the molecule. The plot of the orbital of the excess electron in the anion at an intermediate distance is also shown. Calculations at ωB97x/cc-pvtz level of theory.

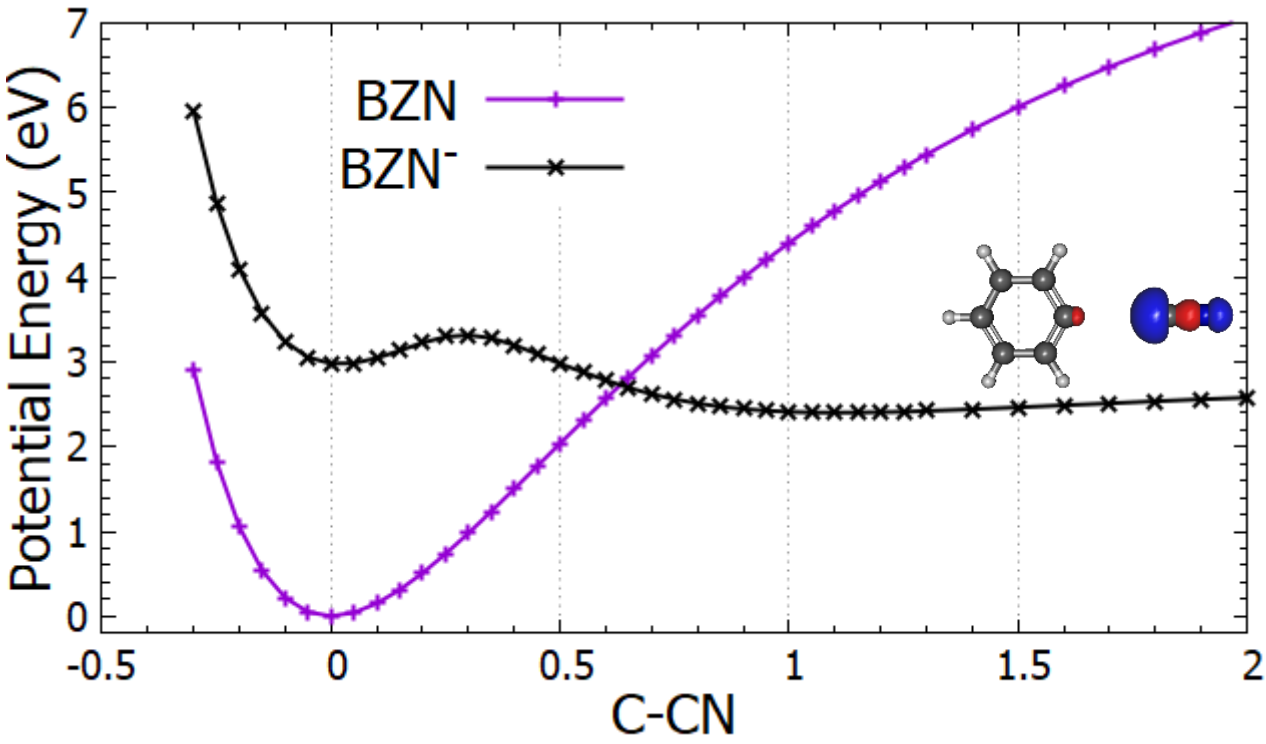

FIGURE 4: Calculated attachment energies (in eV) relative to the neutral ground state of BZN are given together with the molecular orbitals involved in the trapping of the extra electron. Core-excited states are also obtained at 4.48, 5.12, 5.40, and 5.74 eV (not shown in the figure).

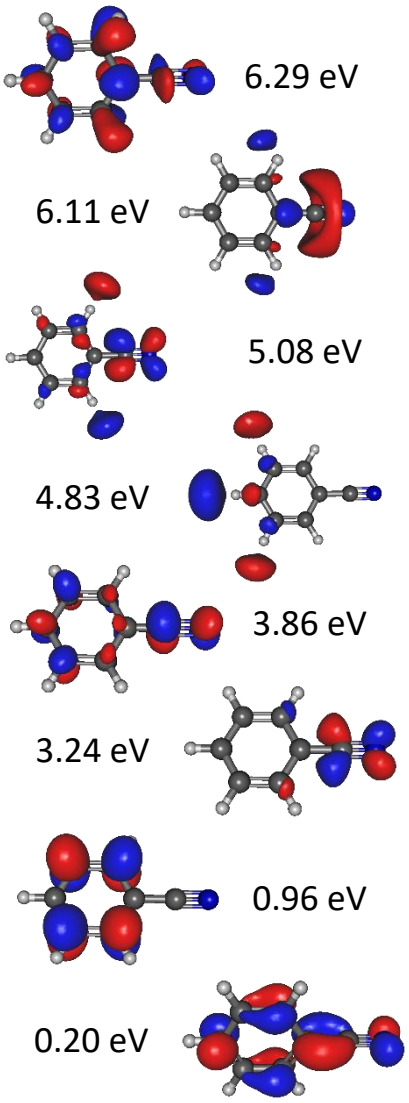

Figure 5: Temperature dependence of the CN^- and Cl^- anion yields (full circles and open squares, respectively) recorded at the electron accelerating voltage of 0.9 V (i.e., 0.5 eV). The dashed line is a guide-to-the-eye.

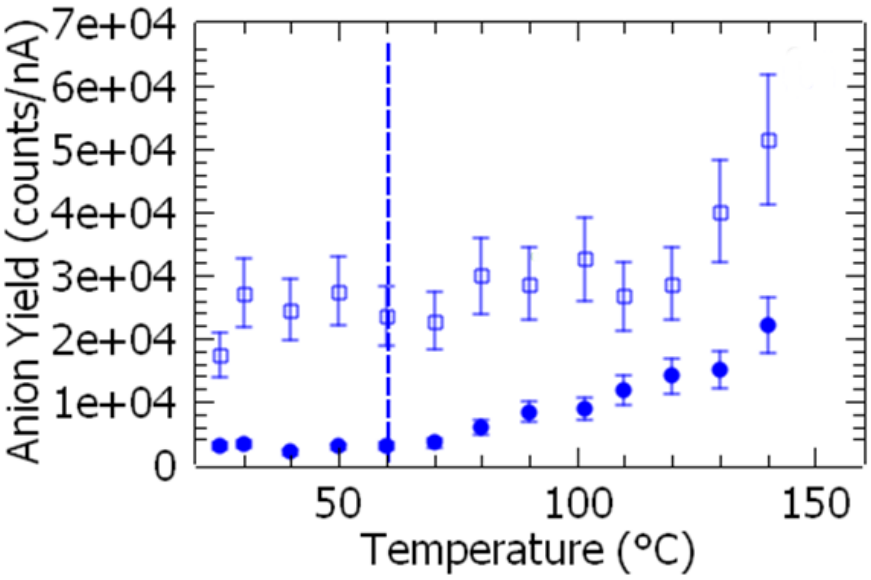

IX. REFERENCES

1 https://www.atamanchemicals.com/benzonitrile_u27521/

2 B.A. McGuire, A.M. Burkhart, S. Kalenskii, C.N. Shincledecker, A.J. Remijan, E. Herbst, M.C. McCarthy, Detection of the aromatic molecule benzonitrile (c-C6C5CN) in the interstellar medium, *Science* 359 202-205 (2018).

3 U. Jacovella, J.A. Noble, A. Guliani, C.S. Hansen, A.J. Trevitt, J. Mouzay, I. Couturier-Tamburelli, N. Pietri, L. Nahon, Ultraviolet and vacuum ultraviolet photo-processing of protonated benzonitrile (C6H5CNH+), *A&A* 657 A85 (2022).

4 T.S. Cantrell Photochemical cycloaddition of benzonitrile to alkene. Factor controlling the site addition, *J. Org. Chem.* 42 4238

5 B.A. McGuire, R.A. Loomis, A.M. Burkhart, K.L.K. Lee, C.N. shingledecker, S.B. Chamley, I.R. Cooke, M.A. Cordiner, E. Herbst, S. Kalenskii, M.A. Siebert, E.R. Willis, C. Xue, A.J. Remijan, M.C. McCarthy, Detection of two interstellar polycyclic aromatic hydrocarbon via spectral matched line, *Science* 371 1265-1269 (2021).

6 J.-I. Aoyama, K. Tabayashi, K. Saito, Dissociative excitation of benzonotrile by ultraviolet multiphoton absorption, *J. Photochem. Photobiol A: Chemistry* 172 241-249 (2005).

7 1.5x104 electrons per deposited 500keV. ICRU report 31, Average energy recquired to produced an ion pair, International Commission of Radiation Units and Measurements, Bethesda (1979).

8 M. Mücke, M. Braun, S. barth, M. Förstel, T. Lischke, V. Ulrich, T. Arion, U. Becker, A. Bradshaw, U. Hergenhahn, A hitherto unrecognized source of low-energy electron in water, *Nat. Phys.* 6 146-146 (2010).

9 C.R. Arimainayagam, R.T. Garrod, M.C. Boyer, A.K. Hay, S.T. Bao, J.S. Campbell, J. Wang, C.M. Novak, M.R. Arumainyagam, P.J. Hodge, Extraterrestial prebiotic molecules: photochemistry vs. radiation chemistru of interstellar ices, Chem.Soc.Rev. 48 2293-2314 (2019).

10 H. Abdoul-Carime, B. Lathuilère, P. Nédelec, J. Kopyra, Synthesis of benzene and phenol induced from the irradiation of benzonitrile:water ices by low energy (< 10 eV) electrons, *J. Geophys. Res. Planets* 129 e2023JE008151 (2024).

11 E. Böhler, J. Warneke, P. Swiderek, Control of chemical and synthesis by low energy electrons *Chem Rev. Soc*. 42 9219-9231 (2013).

12 H. Abdoul-Carime, I. Bald, E. Illenberger, J. Kopyra, Selective Synthesis of Ethylene and/or Acetylene from Dimethyl Sulfide Controlled by Slow Electrons, *J.Phys.Chem C* 122 24137 (2018).

13 M.C.Boyer, N. Rivas, A.A. Tran, C.A. Verish, C.R. Arumaingayam, The role of low energy (<20 eV) electrons in astrochemstry, Surf. Sci. 652 26-32 (2016).

14 Abdoul-Carime H., Bald I., Illenberger E., Kopyra J., 2018, Selective synthesis of ethylene and/or acetylene from dimethyl sulfide controlled by slow electrons, *J. Phys. Chem. C.* 122 24137-24141.

15 Y. Zhang, S. He, W. Guo, Y. Hu, J. Huang, J.R. Mulcahy, W.D. Wei, Surface Plasmon driven hot-electron photochemistry *Chem. Rev.* 118 2927-2954 (2018).

16 Kinetics and Mechanism of Plasmon-Driven Dehalogenation Reaction of Brominated Purine Nucleobases on Ag and Au, *ACS Catalys.* 11(13), 8370-8381 (2021),

17 J.Y Park, S.M. Kim, H. Lee, I.I. Nedrygailov, Hot electron mediated surface chemistry: toward electronic control of catalytic activity, *Acc. Chem. Res.* 48 2475-2483 (2015).

18 S. Mukherjee, F. Libish, N. Large, O. Neumann, L.V. Brown, J. Cheng, J.B. Lassiter, E.A. Carter, P. Nordlander, N.K. Halas, Hot electron do the impossible: plasmon induced dissociation of H2 on Au, NanoLett. 13 240-247 (2013).

19 S. Kogokoski, J. Ameixa, A. Mostafa, I. Bald, Lab-on-a-DNA origami: nanosengineered single molecule platform, *Chem.Commun.* 59 4726-4741 (2023).

20 C. Wang, W.-.C. D. Yang, D. Raciti, A. Bruma, R. Marx, A. Agrawal, R. Sharma, Endothermic reaction at room temperature enable by deep ultraviolet plasmon, *Nat. Mat.* (2021).

21 M. Barnardi, J. Mustafa, J.B. Neaton, S.G. Louie, Theory and computation of hot carriers generated by surface plasmon resonance in noble metal, *Nature Commun.* 6 7044 (2015).

22 D.D. Blackwell, F.F. Chen, Time resolved measurements of the electron energy distribution function in helicaon plasma, Plasma Sources Sci Technol. 10 226-235 (2001).

23 D. Sarangi, A. Karimi, Comparative study of carbon nanotubes grown over metallic wire by cold plasma assisted technique, *Carbon* 42 1113-1118 (2004).

24 M. Heni, E. Illenberger, Electron attachment by saturated nitriles, acrylonitrile (C_2H_3CN) and benzonitrile (C_6H_5CN*), Int. J. Mass Spectrom. Ion Proc*. 73 127-144 (1986).

25 G. Thiam, F. Rabilloud, Multi-basis-set (TD-)DFT methods for predicting electron attachment energies, *J.Phys.Chem. Lett.* 12 9995-10001 (2021).

26 S. Denifl, S. Ptasinska, M. Cingel, S. Matejcik, P. Scheier, T.D. Märk, Electron attachment to the DNA bases thymine and cytosine, *Chem. Phys. Lett.* 377 74-80 (2003).
27 R.A. Kendall, T.H. Dunning Jr., R.J. Harrison Electron affinities of the first-row atoms revisited. Systematic basis sets and wave functions, *J. Chem. Phys*. 96 6796-6806 (1992).
28 J. Chai, M. Head-Gordon Systematic optimization of long-range corrected hybrid density functionals, *J. Chem. Phys*. 128, 084106 (2008).
29 M. J. Frisch, et al., Gaussian 16, Revision C.01, Gaussian, Inc., Wallingford CT, 2016.
30 A.-R. Allouche, A. Gabedi User Interface for Computational Chemistry Softwares, *J. Comput. Chem.* 32, 174-182 (2011).
31 H.Abdoul-Carime, F. Mounier, F. Charlieux, H. André, Correlated ion-(ion-neutral) time-of-flight mass spectrometer, *Rev. Sci. Instrum.* 94 045104 (2023).
32 F. Charlieux, H. Abdoul-Carime, Processes induced by electrons at sub-ionization energies studied by the correlated ion-(Ion/neutral) mass spectrometry, Chem.Phys.Chem. DOI :10.1002/cphc.202200722 (2023).
33 S. Gohlke, H. Abdoul-Carime, E. Illenberger, Dehydrogenation of adenine induced by slow (<3eV) electrons, *Chem.Phys.Lett.* 380 595-599 (2003).
34 S. Matejcik, A. Kiendler, A. Stamatovic, T.D. Märk, A crossed beam hig resolution study of dissociative electron attachment to CCl4, *Int. J. Mass. Spectrom. Ion Proc.* 149/150 311-319 (1995).
35 E. Illenberger, J. Momigny in Gaseous molecular ions: an introduction to elementary processes induced by ionization, H. Baümgartel, E.U. Franck, W. Grünbein, (Etds), Springer Verlag Berlin Heidelberg (1992).
36 T.F. O'Malley, Theory of dissociative attachment, Phys. Rev. 150 14-29 (1966).
37 A.M. Scheer, K. Aflatooni, G.A. Gallup, P.D. Burrow, Bond beaking and temporary anion states in uracil and halouracils: implication for the DNA bases, Phys. Rev. let. 92 0681002 (2004).
38 T. Sommerfeld, dipole-bound states as doorways in (dissociative) electron attachment, J. Phys. Conf. series 4 245-250 (2005).
39 P.D. Burrow, A.E. Howard, A.R. Johnson, K.D. Jordan, Temporary anion state of HCN, CH_3CN, $CH_2(CN)_2$, selected cyanoethylenes, benzonitriles and tetracyanoquinodemethane, J. Phys.Chem. 96 7570-7578 (1992).
40 S.Denifl, S. Ptasinska, M. Probst, J. Hrusak, P. Scheier, T.D. Märk, Electron attachment to gas phase DNA base cytosine and thymine, *J. Phys. Chem. A* 108 6562-6569 (2004)

41 S. Gohlke, H.Abdoul-Carime, E. Illenberger, Dehydrogenation of adenine induced by slow (<3 eV) electrons, Chem.Phys.Lett. 380 595-599 (2003).

42 H. Abdoul-Carime, S. Gohlke, E. Illenberger, Site-specific dissociation of DNA bases by slow electrons at early stage of irradiation, *Phys. Rev. Lett. 92*, 168103 (2004).

43 J.C. Rinstra-Kiracofe, G.S. Tschumper, H.F. Schaeffer III, S. Nandi, G.B. Ellison, Atomic and molecular electron affinities: photoelectron experiments and theoretical computations, *Chem.Rev.* 102 231-282 (2002).

44 K. Regeta, S. Kumar, T. Cunha, M. Mendes, A.I. Lozano, P.J.S. Pereira, G. Garcia, A.M.C. Moutinho, M.-. Bacchus-Montabonel, P. Limão-Vieira, Combined experimental and theoretical studies on electron transfer in potassium collision with CCl_4, *J. Phys.Chem. A* 124 3220-3227 (2020).

45 S. Matejcik, V. Foltin, M. Stano, J.D. Skalny, Temperature dependencies in dissociative electron attachment to CCl_4, CCl_2F_2, $CHCl_3$ and $CHBr_3$, *Int.J. Mass Spectrom.* 223-224 9-19 (2003).

46 G. Caldwell, T.F. Magnera, P. Kabarle, S_N2 reactions in the gas phase. Temperature dependence of the rate constants and energies of the transition states. Comparison with solution, *J. Am. Chem. Soc.* 106 959-960 (1984).

47 Chlorobenzene market forecast (2024-2026), Industry ARC – Analytic Reserach Consulting, https://www.industryarc.com/Report/17893/chlorobenzene-market.html

48 F. Temerov, K. Pham, P. Juuti, J.M. Mäkelä, E. Grachova, S. Kumar, S. Eslava, J.J. Saarinen, Silvar-decorated TiO_2 inverse opal structure for visible light induced photocatalytic degradation of organic pollutants and hydrogen evolution, *ACS Appl. Mat. Interf.* 12 41200-41210 (2020).

49 K. Zhang, Z. Xi, Z. Wu, G. Lu, X. Huang, Visible light induced selective oxidation of amines into imines over UiO66-NH_2@Au@COF core shell photolysis, *ACS Sustain. Chem. Eng.* 9 12623-12633 (2021).

50 O.A. Mbrouk, M. Fawzy, H.M. Elshafey, M. Saif, H. Hafez, M.S.S. Abdel Mottaleb, Green synthesis plasmonic Pd-ZnO nanomaterials for visible light induced photobiogas production fromindustrial wastesater, *Appl. Organometal. Chem.* 36 e6807 (2022).

51 S.Müller, E. Ströfer, M. Kohns, K. Münnemann, E. von Harbour, H. Hasse, Investigation of partial oxidation of methane in a cold plasma reactor with detailed product analysis, *Plasma Chem Plasma Process.*, 43 513-532 (2023).

Dissociation of benzonitrile induced by low energy electrons: a combined theoretical and experimental study

H. Abdoul-Carime [1*], Guillaume Thiam [2], Franck Rabilloud [2]

[1] Université de Lyon, Université Lyon 1, Institut de Physique des 2 Infinis, CNRS/IN2P3, UMR5822, F-69003 Lyon, France

[2] Université de Lyon, Université Claude Bernard Lyon 1, CNRS, Institut Lumière Matière, UMR5306, F-69622 Villeurbanne, France

*Corresponding author: hcarime@ipnl.in2p3.fr

SI1: (a) The mass spectrum of ionized benzonitrile vapor with electron energy of ~11 eV for which the cation distribution can be compared to the NIST reference [1]. In this measurement, EG1 is in "OFF" mode. (b) Mass spectrum of anion produced from the collision of the electron accelerated at 2.8 V from EG1 (EG2 is "OFF"). A unique anion fragment is observed at m/z 26.

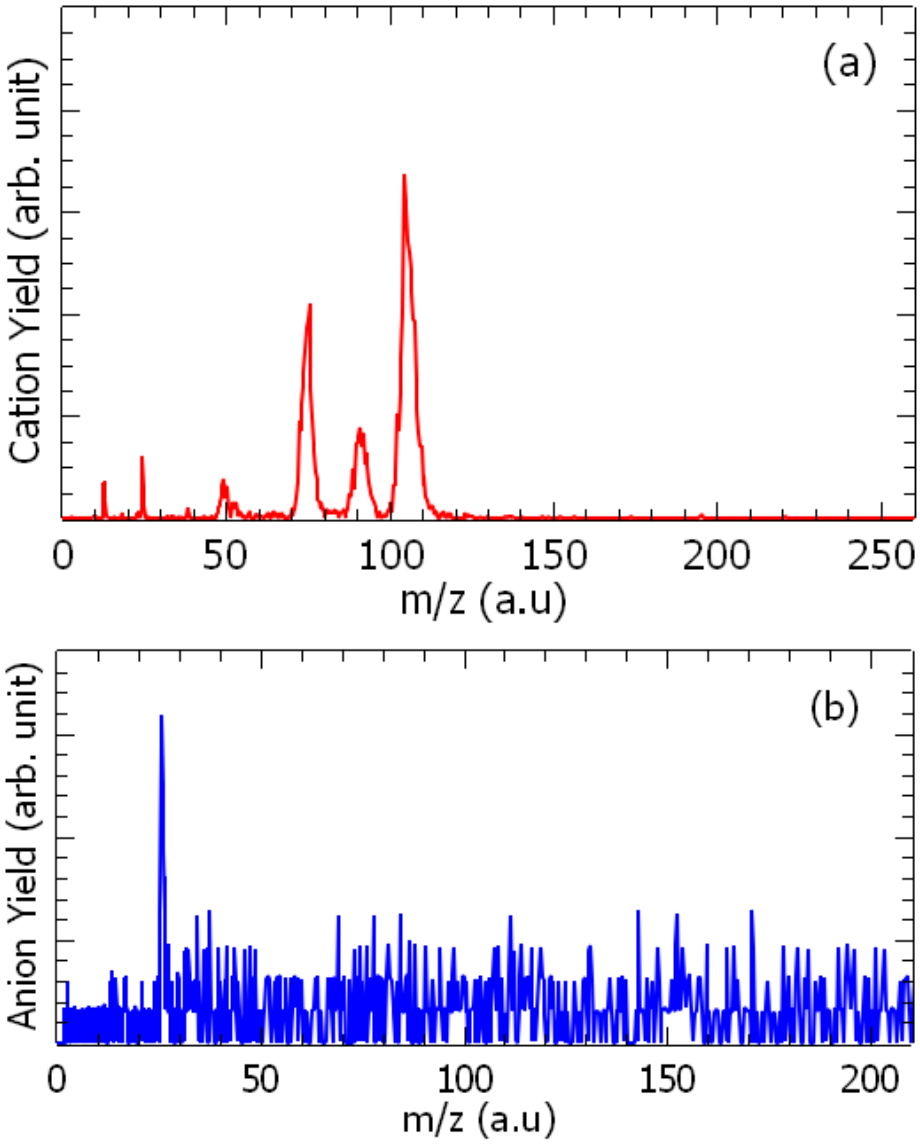

SI2: The CN^- anion yield as the function of the electron accelerating voltage (AV1). The incident electron energy is obtained by subtracting 0.4 eV to AV1 (see text). The numbers provided in the figure are the electron energy. The smooth purple solid line is the cumulative Gaussian fit to the data and the dashed lines are the individual Gaussian function.

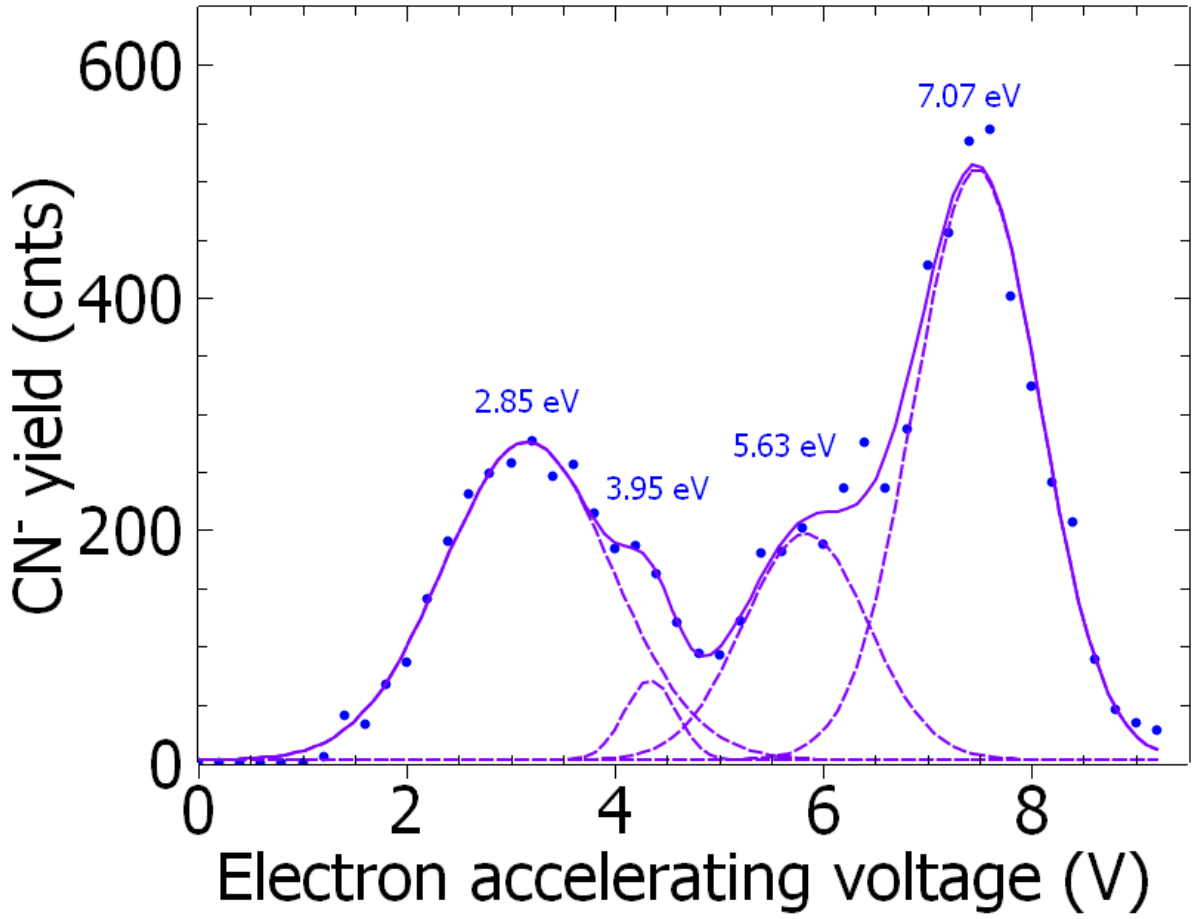

SI3: Cation mass spectrum recorded from the 3.5 V accelerated electron impact on an admixture of CCl_4-BZN vapor. The neutral species are ionized by ~12 eV electrons produced by EG2. Peaks at m/z 103 and 117 are identified to BNZ^+ and CCl_3^+, the latter arising from the "ionization" of CCl_4 [1]. The m/z 113 and 77 may be attributed to C_6H_5Cl (chlorobenzene) and C_6H_5 species respectively. The m/z 108 may be attributed to CCl_2CN^+, from trichloroacetonitrile CCl_3CN, in agreement with the NIST ionization mass spectrum [1]. Both the chlorobenzene and the trichloroacetonitrile are very likely to arise from the Cl^- and CN^- ion reaction with BZN and CCl_4, respectively. The ~12 eV electron ionizing energy corresponds almost to the ionization potential of CCl_4 (11.5 eV)[1], BZN (9.7 eV) [1], CCl_3CN (11.89) [1] and C_6H_5Cl (9.08 eV) [1].

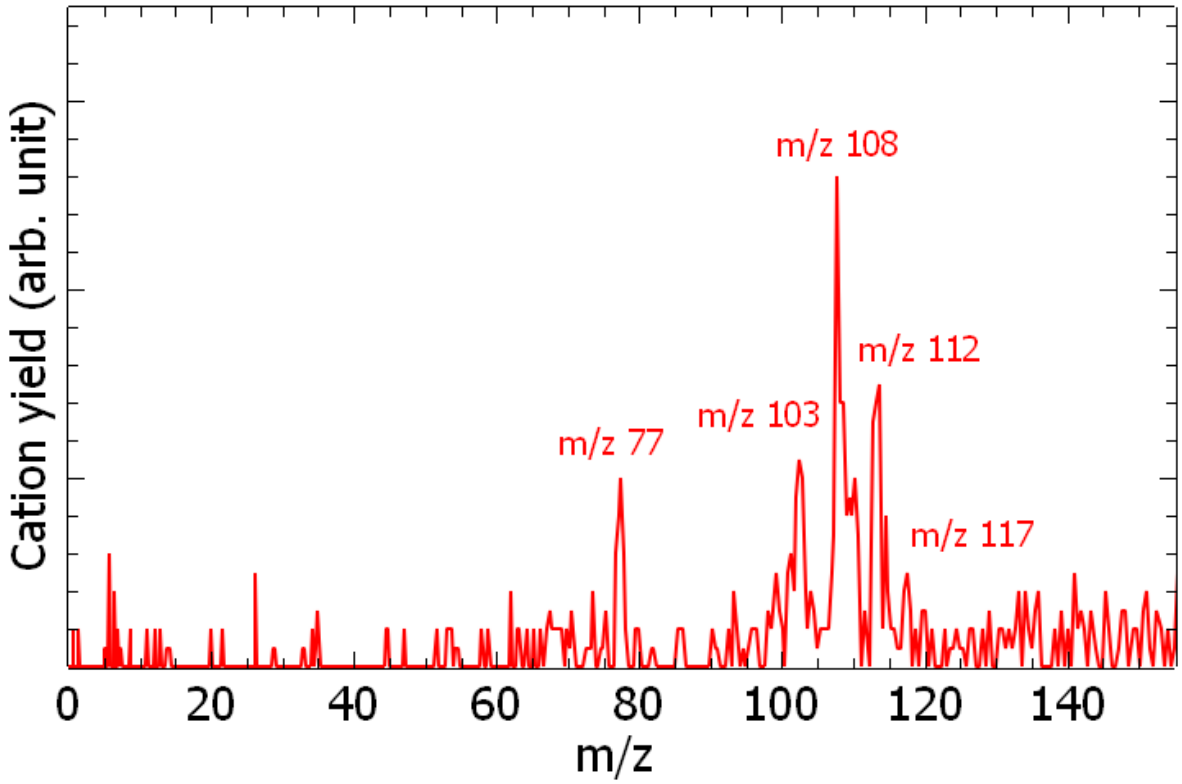

[1] NIST data webbook.